



Pulsed Nd:YAG Laser Welding of Cardiac Pacemaker Batteries with Reduced Heat Input

Variations in pulsing parameters are shown to reduce glass-to-metal seal temperatures

BY P. W. FUERSCHBACH AND D. A. HINKLEY

ABSTRACT. The effects of Nd:YAG laser beam welding process parameters on the resulting heat input in 304L stainless steel cardiac pacemaker batteries have been studied. By careful selection of process parameters, the results can be used to reduce temperatures near glass-to-metal seals and assure hermeticity in laser beam welding of high reliability components. Three designed response surface experiments were used to compare welding performance with lenses of varying focal lengths. The measured peak temperatures at the glass-to-metal seals varied from 65° to 140°C (149° to 284°F) and depended strongly on the levels of the experimental factors. It was found that welds of equivalent size can be made with significantly reduced temperatures. The reduction in battery temperatures has been attributed to an increase in the melting efficiency. This increase is thought to be due primarily to increased travel speeds, which were facilitated by high peak powers and low pulse energies. For longer focal length lenses, weld fusion zone widths were found to be greater even without a corresponding increase in the size of the weld. It was also found that increases in laser beam irradiance either by higher peak powers or smaller spot sizes created deeper and larger welds. These gains were attributed

to an increase in the laser energy transfer efficiency.

Introduction

Pulsed Nd:YAG laser beam welding is widely used for final closure of small high reliability components such as cardiac pacemaker batteries or electromechanical relays. The process is regarded to be ideally suited for these applications since it can deliver a small and precise amount of welding energy in a very tiny spot. Many of these components contain glass-to-metal seals that can be cracked by thermally induced strains during welding. Relative to traditional arc welding processes, the laser beam welding (LBW) process is believed to minimize the ther-

mal energy input to the part and thereby assure a hermetic closure (Ref. 1).

The Nd:YAG laser pulses at a high repetition rate and creates a continuous seam weld of overlapping spots. Unlike CO₂ gas lasers, the pulsed Nd:YAG solid-state laser produces very high peak powers relative to the average power of the laser. A typical pulsed Nd:YAG laser with an average power rating of 400 W can reach a peak power in a 3-ms pulse as high as 8000 W. Because of these high peak powers, under most processing conditions, the weld pool solidifies so quickly after each pulse that the resulting steep thermal gradients create solidification cracking defects in materials that are readily weldable with other processes (Refs. 2, 3). However, the unique advantages of the pulsed Nd:YAG laser welding process are considerable and have assured its continued application. Low-power operation, deep weld penetration, enhanced absorption, high melting efficiency, and fiber delivery are just some of the advantages attributed to this welding process (Ref. 4).

The technical challenge in welding with pulsed Nd:YAG LBW is identifying the set of processing parameters necessary to make a high-quality, low heat input, hermetic weld. Recommended practices usually do not clearly define the roles of the individual process factors in predicting penetration, absorption, and heat input (Refs. 5-7). The task of selecting an ideal weld schedule for the more basic continuous wave laser is in it-

KEY WORDS

Pulsed Nd:YAG
Pacemaker
Medical Battery
Glass-to-Metal Seal
Response Surface
Melting Efficiency
304L Stainless Steel
Hermeticity
High Reliability
Heat Input

P. W. FUERSCHBACH with Sandia National Laboratories, Albuquerque, N. Mex. and D. A. HINKLEY formerly with Wilson Greatbatch Ltd., Clarence, NY, is with Square D Company, Lincoln, NE.

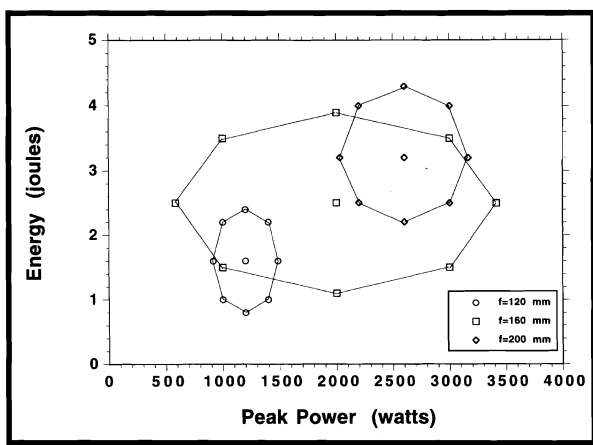


Fig. 1 — Range of experimental factors, indicating the three overlapping star-shaped designs.

self problematic when one considers such singular factors as laser mode or optic F number. However, with the pulsed Nd:YAG laser, additional factors such as peak power, pulse duration, pulse repetition rate, pulse overlap, and pulse energy all become important and must be considered in weld schedule development. These factors are in addition to the traditional laser weld schedule parameters such as average power, travel speed, and spot size.

enlarged melt volumes or 2) reduced heat conduction into the base metal and resulting enlarged melt volumes. While both factors serve to increase process efficiency, the effect of each on the temperature at a heat sensitive feature can be opposite. In other words, if one selects parameters to increase process efficiency, a corresponding increase in melting efficiency (ratio of the melted volume enthalpy to the energy absorbed by the workpiece) is not certain. An indepen-

dent measurement of heat input is required to determine the role of process parameters on melting efficiency and reduce heat input. Clearly, with the pulsed Nd:YAG laser process, the potential for interactions among the process parameters is high and experiments to distinguish the role of each factor can very easily become impractical. Designed statistical experiments such as fractional factorials are often employed to optimize manufacturing processes in applications like this where the number of experimental factors is large and unwieldy. The use of these statistical experiments in research applications can be disappointing if, at the end, the results do not clearly indicate how and why a factor is important.

For pulsed Nd:YAG laser spot welds, Liu, *et al.* (Ref. 8), has correlated the process efficiency (ratio of the melted volume enthalpy to the incident laser power intensity. However, process efficiency measurements cannot be used to reduce base metal heat input because energy transfer efficiency is usually an uncontrolled variable in most experiments (Ref. 9). An increase in process efficiency can be due to either 1) an increased energy absorption and

dent measurement of heat input is required to determine the role of process parameters on melting efficiency and reduce heat input. Clearly, with the pulsed Nd:YAG laser process, the potential for interactions among the process parameters is high and experiments to distinguish the role of each factor can very easily become impractical. Designed statistical experiments such as fractional factorials are often employed to optimize manufacturing processes in applications like this where the number of experimental factors is large and unwieldy. The use of these statistical experiments in research applications can be disappointing if, at the end, the results do not clearly indicate how and why a factor is important.

It was the goal of this work to use response surface methods (Ref. 10) in a manner that distinguishes the primary effects of specific process parameters in pulsed Nd:YAG laser welding. By careful experimental design, we can *a priori* select the process parameters that most influence the responses to observe, and thereby more clearly study, the interaction of the process parameters. This experimental approach serves to not only optimize a specific process application but also to increase our physical understanding for other applications of the process. The response surface experiments were intended to determine how laser weld process parameters could be selected to minimize temperatures near the glass-to-metal seal of a cardiac pacemaker battery. The weld development was undertaken in support of a new high reliability production operation.

Experimental Approach

The levels of the process parameters used in the experiment are given in Table 1. The three factors chosen to be varied in the experiment are laser pulse energy, peak power, and lens focal length (which effectively varies the focus spot size). In early screening experiments, it was found that, for a given lens, satisfactory welds could not be made with the same levels of peak power and pulse energy that proved satisfactory with one of the other two focusing lenses. This was primarily due to the occurrence of spatter and excessive penetration that yielded welds that would not be acceptable. As a consequence, a separate design of the same type was used for each lens. Each experimental design type is a star-shaped central composite design — Fig. 1. Even though separate experiments were necessary with each of the lenses, one can see from the figure that there still is some

Table 1 — Pulsed Nd:YAG Laser Welding Parameters

Energy (J)	Peak Power (W)	Frequency (pps)	Pulse Width (ms)	Travel Speed (mm/s)	No. of Samples
120-mm focal length/estimated spot size is 0.45 mm					
1.0	1000	200	1.0	25.4	2
1.0	1400	200	0.7	25.4	2
2.2	1000	91	2.2	14.0	2
2.2	1400	91	1.6	14.8	2
0.8	1200	266	0.6	33.9	2
2.4	1200	82	2.0	14.0	2
1.6	917	125	1.7	16.5	2
1.6	1483	125	1.1	20.7	2
1.6	1200	125	1.3	19.1	3
160-mm focal length/estimated spot size is 0.6 mm					
1.5	1000	133	1.5	2.1	2
1.5	3000	133	0.5	27.1	2
3.5	1000	57	3.5	11.4	2
3.5	3000	57	1.2	12.3	2
1.1	2000	184	0.5	27.9	2
3.9	2000	51	2.0	10.6	2
2.5	586	80	4.3	12.7	2
2.5	3414	80	0.7	17.8	2
2.5	2000	80	1.2	14.4	3
200-mm focal length/estimated spot size is 0.75 mm					
2.5	2200	80	1.1	15.7	2
2.5	3000	80	0.8	15.7	2
4.0	2200	50	1.8	10.6	2
4.0	3000	50	1.3	11.0	2
2.2	2600	91	0.8	17.8	2
4.3	2600	46	1.7	10.2	2
3.2	2034	62	1.6	12.7	2
3.2	3166	62	1.0	12.7	2
3.2	2600	62	1.2	12.7	3

Note: All welds were performed at 200 W average power.

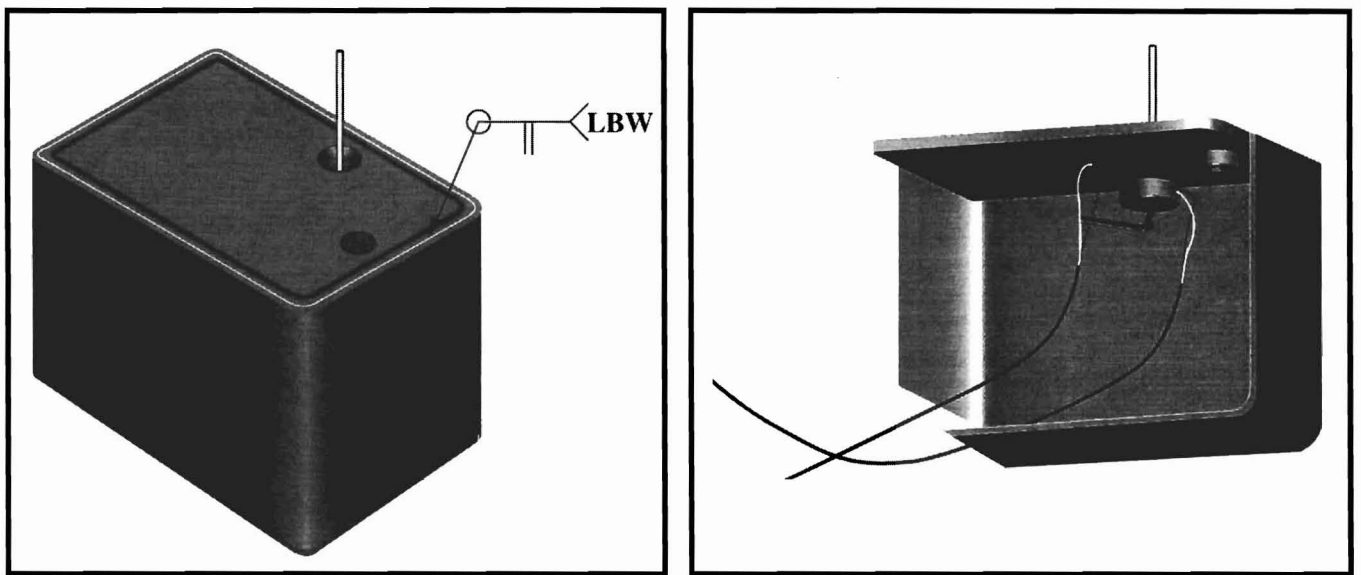


Fig. 2 — Cardiac pacemaker battery, showing the location of the weld joint and placement of thermocouples.

overlap among the three experiments. Response surface analyses were necessarily run separately for each of the three experiments, but comparisons among the results of each experiment were made when warranted.

It is known that the depth of weld penetration is dependent on the laser beam irradiance (power per unit area). For pulsed laser welding, the beam irradiance is determined both by the peak power during a laser pulse and by the spot size of the focused laser beam. The peak power (P_p) is found by dividing the pulse energy (E) by the pulse duration (t_p) as shown below:

$$P_p = E/t_p$$

One can see from this expression that, by varying the pulse duration, independent levels of peak power for a given pulse energy can be obtained. This approach was used to set the specific levels of peak power shown in Table 1.

It has been demonstrated that the average power of a pulsed solid-state laser has a significant effect on the laser spot size (Ref. 11). As the laser power increases, thermal gradients are created in the laser rod that distort its shape and influence the focused spot size obtained with a given focusing lens. To prevent biased experimental results due to an uncontrolled variable, the average power was fixed at 200 W for all welds. This step assured that the only factor that could affect spot size in the experiment is the change in focusing lens. The three lens focal lengths chosen for the experiment are typical lengths used for welding

with this type of laser. It is well-known that the focused laser spot size is proportional to the focal length; therefore the three lenses chosen were expected to yield three different laser beam spot sizes. Approximate values of spot size diameter as furnished by the laser manufacturer are given in Table 1.

The average power (P) is calculated from the product of the pulse frequency (f) and the pulse energy (E) as follows:

$$P = fE$$

Since the pulse energy is a variable in

the experiment, the pulse frequency was adjusted to maintain an average power of 200 W. The levels of pulse frequency used in the experiment are given in Table 1. A variable pulse frequency will necessarily affect pulse overlap. To prevent impractical welds with inconsistent root penetration or with excessive numbers of pulses, it is necessary to maintain a constant pulse overlap. The pulse overlap was held constant at 75% by adjusting the travel speed. This overlap was calculated by measuring the width of individual spot welds that were made for each experimental condition and then calcu-

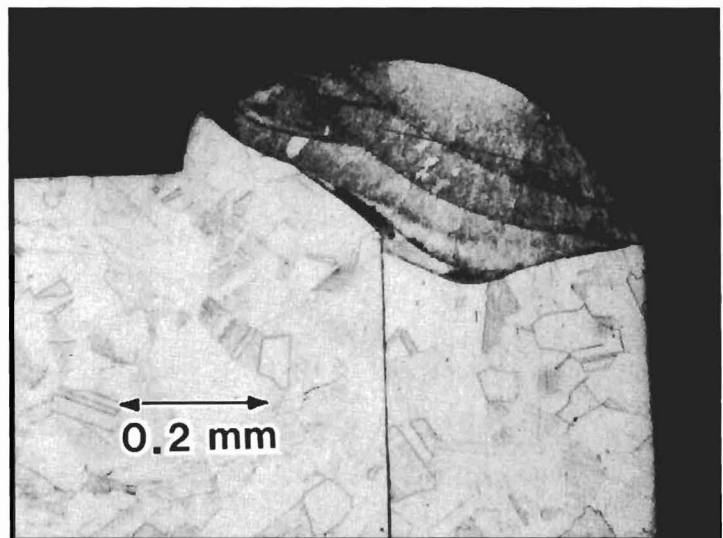


Fig. 3 — Typical cross section of pulsed Nd:YAG laser welded battery, showing edge weld joint on 304L stainless steel, $f = 120$ mm.

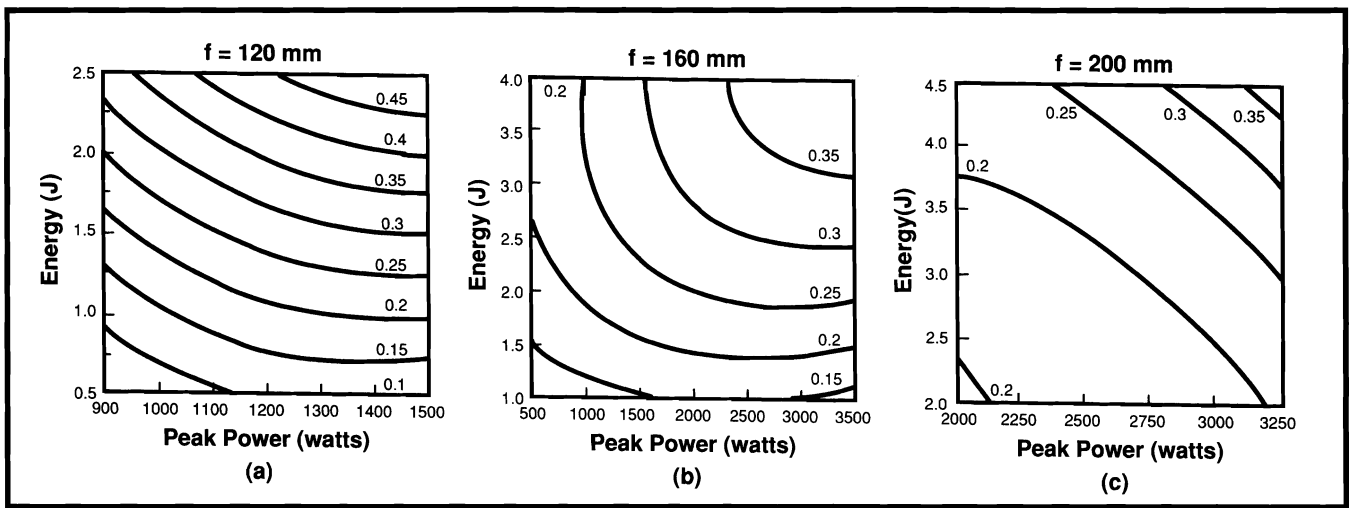


Fig. 4 — Contour plots showing the effect of peak power and pulse energy on weld penetration for three lenses; A — $f = 120$ mm, $R^2 = 0.99$; B — $f = 160$ mm, $R^2 = 0.88$; C — $f = 200$ mm, $R^2 = 0.91$.

lating the required travel speed v from the following formula:

$$v = (D - L') f$$

where D is the measured pool diameter and L' is the overlap length. The overlap length is the product of the specified fractional pulse overlap and the measured pool diameter.

All of the laser welds in the experiment were made with a Lumonics JK702H, 350-W pulsed Nd:YAG laser. The laser beam was transmitted to the workstation through a 600- μ m-diameter (0.002-in.-diameter), 60-m-long (197-ft-long) fiber. The parts were moved under the beam with a Unidex 21 CNC motion control system. The CNC maintained the part travel speed and controlled the laser beam shutter open time. Laser pulse energy, frequency, and pulse duration were also set and controlled with the CNC.

Laser average power was measured in the workstation below the focusing lens using a Coherent LM1000 power meter. Actual production grade battery cases and headers were used for the experiments. Both parts were made from 304L stainless steel. The header is attached to the case with an edge weld joint that was welded in a single pass. The batteries did not contain any electrolyte.

Welds were made with the surface of the weld joint at the beam waist position where the greatest weld depth was obtained. The approximate waist position of the minimum spot size for a particular focusing lens was determined by making a series of single pulse exposures on Kapton film at 0.010-in. (0.254-mm) increments below the focusing lens near the focal plane. The diameter of the drilled holes in the Kapton film was measured under a microscope. The minimum waist position was finalized by making a series

of bead-on-plate welds about the sharp focus position determined from the Kapton film, measuring the depth of penetration and selecting the center position where the deepest penetration was obtained.

Thermocouple measurements were made in two places on the battery to observe the effect of experimental factors on the thermal input to the battery. Type K thermocouples with a 0.25-mm (0.01-in.) diameter were used. One thermocouple was attached directly to the glass-to-metal seal ferrule, and one thermocouple was attached to the center of the header — Fig. 2. A special fixture was fabricated and assured that the thermocouples were resistance welded in the same location on each battery. The time vs. temperature traces were recorded on an IBM-compatible PC through a 12-bit A/D board.

Weld penetration was defined as the vertical distance melted at the weld joint interface and was determined from the average of four metallographic cross sections. Area measurements of the fusion zone were made with a planimeter from the average of two metallographic cross sections.

Results and Discussion

Penetration and Absorption

All of the welds made in the experiment are of relatively shallow penetration and may be described as conduction mode welds. While certainly attainable with this laser, no deep finger-like penetration welds (*i.e.*, keyhole) were made in this study. The design requirement for joint penetration depth is only 0.20 mm (0.008 in.). A typical weld is shown in Fig. 3. Pulsed laser welds are easily recognized by the solidification ripples visible in the fusion zone, which are due to the overlap of successive laser pulses.

The effect of the peak power and pulse energy on weld penetration depth is shown in the contour plots given in Fig. 4. Each figure represents the contour plot for one of the lenses used in the experiment. One can see that, for each lens, increasing either peak power or pulse energy independently results in increased penetration depth. This effect was clear

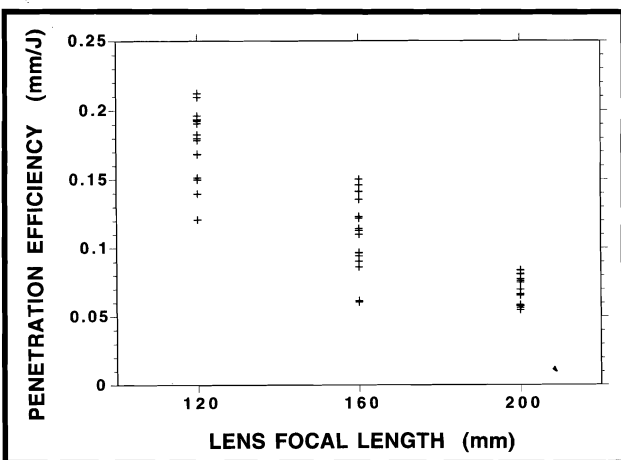


Fig. 5 — Increase in penetration per unit joule of pulse energy that is obtained with short focal length lenses.

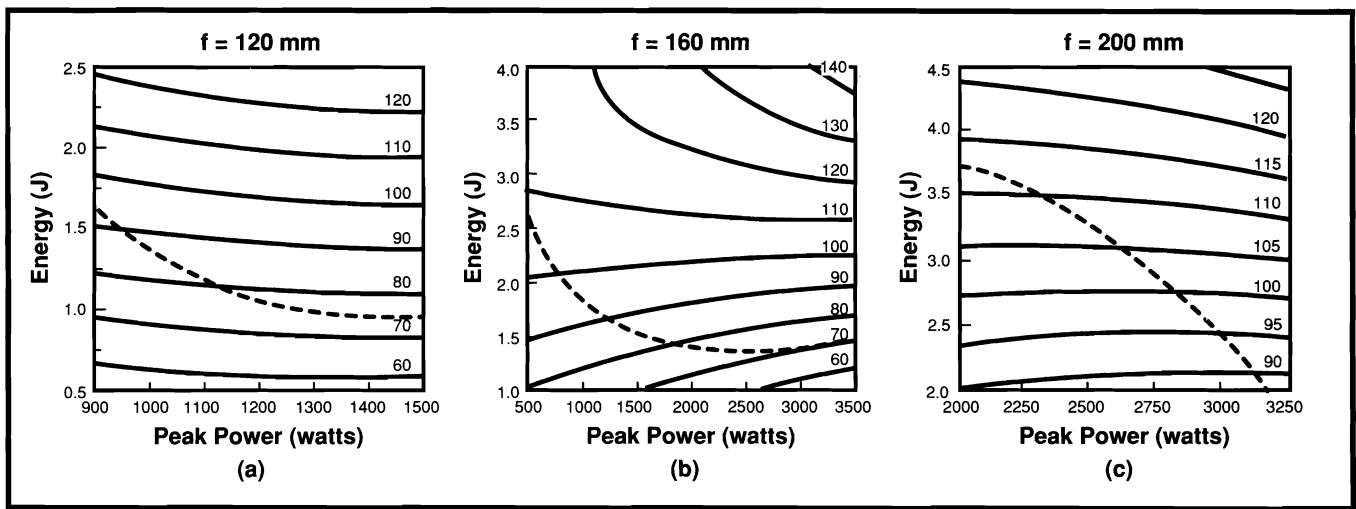


Fig. 6—Contour plots showing the effect of peak power and pulse energy on thermocouple temperatures ($^{\circ}\text{C}$). The dashed line represents the contour line for constant penetration = 0.2 mm as in Fig. 4. A — $f = 120$ mm, $R^2 = 0.98$; B — $f = 160$ mm, $R^2 = 0.95$; C — $f = 200$ mm, $R^2 = 0.96$.

during the initial screening experiments and was used to adjust the peak power and pulse energy to assure that a penetration depth of 0.2 mm was obtained for each lens. The selection of factor levels also placed 0.2 mm near the middle of the experimental range. These results are consistent with Nd:YAG spot-weld measurements (Refs. 2, 8) where increases in pulse energy or peak power resulted in greater weld pool volumes.

The deeper penetration that results from an increased pulse energy, as shown in Fig. 4, is due to an increase in the total laser energy input per length of weld. It is important to note that, since average power was held constant, the decreased pulse frequency necessary with high pulse energy required a slower travel speed to maintain consistent pulse overlap. As a result, the heat input per unit length of weld increased as pulse energy increased. The slower travel speeds result in greater total energy absorption by the battery and larger, deeper weld pools.

In contrast, for a given pulse energy, increasing peak power results in deeper penetration through greater weld pool vaporization, cavity depression, and absorption per pulse. Unlike pulse energy, the increases in peak power in the experiment did not require a corresponding decrease in travel speed. The deeper penetration is not due to greater energy input per unit length of weld but to more effective utilization of the incident energy. As more metal vaporizes due to the higher radiation flux, the resulting recoil pressure creates a deeper weld pool cavity (Ref. 12). While the mechanism of absorption in this cavity is not fully understood, it has been found that absorption increases with increasing beam irradi-

ance (Refs. 9,13).

Upon careful examination of Fig. 4, one can also see that for equivalent levels of peak power and pulse energy, deeper weld penetration was obtained with the shorter focal length lenses. This result is consistent with an increased beam irradiance one would expect with the shorter focal length. As was the case for peak power, increased irradiance creates greater metal vaporization, more absorption, and deeper weld pools.

It is important to note from Fig. 4 that all three of the independent experimental factors are effective in increasing weld penetration. However, the upper limit for each factor, that is, the level that results in weld pool spatter, is clearly interdependent with the levels of the other factors. The decision as to which factor is best used to increase weld penetration must depend on other considerations and constraints. One such practical consideration is the weld travel speed. If welds are to be made as fast as possible, high pulse repetition rates are needed to assure consistent pulse overlap. Since average power is often limited, high repetition rates can only be achieved by lowering the pulse energy. Figure 4 indicates that, to achieve equivalent weld penetration, pulse energy can be reduced either

by increasing peak power or by using a shorter focal length lens. The enhanced process efficiency that can be obtained by using shorter focal length lenses is illustrated in Fig. 5. The figure shows the increase in weld penetration per unit joule of pulse energy that is obtained as the focal length of the lens decreases. It must be remembered that this increased efficiency did not result in any increased spatter and that all of the welds were of high quality.

Peak Battery Temperatures

The effect of the experimental factors on the measured peak temperatures was quite significant. The peak temperatures ranged from as low as 65°C (149°F) to as high as 140°C (284°F). This large range in measured temperatures was encouraging because it indicated that the experi-

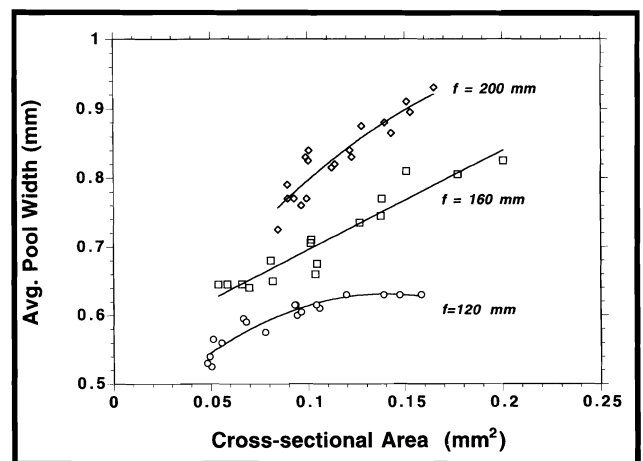


Fig. 7 — Effect of focusing lens on the weld fusion zone width.

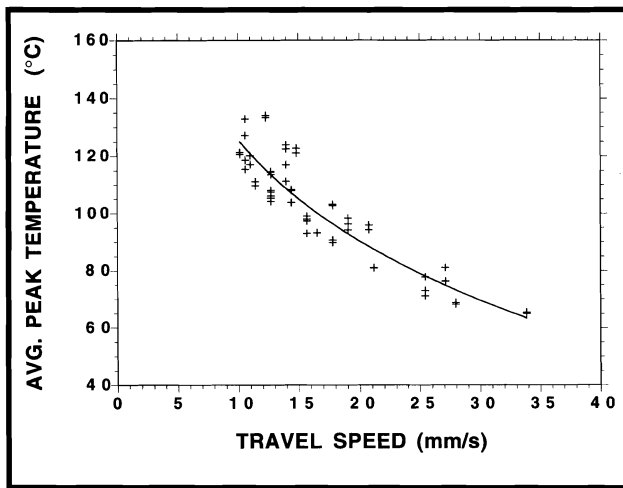


Fig. 8 — Effect of laser welding travel speed on the measured peak temperatures.

mental factor levels were appropriately selected and that process control strategies will likely be effective in reducing battery temperatures. The peak temperatures occurred at different points in time for each condition, but in general the peak temperatures occurred after the weld was finished. It was surprising to find that the ferrule peak temperatures were very close in magnitude to the temperatures on the header since, as shown in Fig. 2, they were located in quite different locations. The two measurements served as a check of each other, and the average of the two measurements was used for the contour plots in Fig. 6.

The contour plots in Fig. 6 show the important effects of the experimental factors on the average peak temperature. One can see that for all lenses and conditions, higher pulse energy results in higher battery temperatures. These increased temperatures are consistent with the fact that the higher pulse energies produced more heat input per unit length of weld. The negative effect of pulse energy on glass-to-metal seal hermeticity has previously been demonstrated (Ref. 11), and the temperature measurements reported here are further corroborating evidence that high pulse energies are detrimental to thermally sensitive components. It is interesting to note that in general, the temperature contours in Fig. 6 do not show the same effect resulting from changes in peak power. For a given average power, peak power is a parameter that can be adjusted without a corresponding effect on temperature. It is also clear from Fig. 6 that, for the welds made with the 200-mm (7.9-in.) focusing lens, the lowest battery temperatures were higher than the lowest temperatures measured with either of the other two

lenses. This result is likely due to the increased minimum pulse energy and corresponding greater heat input that was required with the 200-mm lens.

In addition to the temperature contours in Fig. 6, the figure contains an overlay of the 0.2-mm constant penetration contours that were given in Fig. 4. By tracing along this contour, it is possible to select a processing condition that will result in a low average peak temperature and yet still yields the required 0.2-mm penetration.

When one examines the 0.2-mm weld penetration contours for each of the lenses in Fig. 6, it becomes clear, that to reduce the average peak temperature both high peak powers and low pulse energies are necessary. At the intersection of the 0.2-mm contour with the minimum peak temperatures for the 120-mm (4.7-in.) and 160-mm (6.3-in.) lenses, one can see there is a slight advantage to be gained in processing with the 160-mm lens. As a result, these levels of peak power and pulse energy for the 160-mm lens were chosen as the baseline for weld qualification testing subsequent to this study.

Because of the close similarity in minimum temperatures between the 120-mm and the 160-mm lenses, the decision to select the 160-mm lens was also influenced by other process considerations. As is shown in Fig. 7, the measured weld widths are larger for the longer focal length lenses even at equivalent weld areas. The reason for this effect is due to the larger focused spot size, which creates a wider molten pool but does not significantly increase the overall weld area. A wider weld fusion zone is preferred here because it provides greater tolerance to beam positioning and thereby helps assure hermeticity. In addition, the longer focal length lens is superior in production applications because it provides both a greater depth of focus and a longer working distance.

Another important process consideration is variability due to uncontrollable changes in process variables. It is interesting to note the experimental range of peak power and energy for each of the focusing lenses shown in Fig. 1. As mentioned above, the screening experiments were used to assure that the experimen-

tal range of weld penetration for each lens was approximately consistent with that of the other lenses. The much greater processing range that is apparent for the 160-mm focal length lens is thought provoking. The greater range implies less sensitivity of penetration to process parameter changes. To verify this inference, the polynomial equations that are represented graphically in Fig. 4 were examined. The partial derivatives

$$\frac{\partial D}{\partial E} \quad \text{and} \quad \frac{\partial D}{\partial Pp}$$

of the response surface equation for each lens (where D = depth of penetration) were evaluated at the conditions that produced 0.2-mm penetration and the lowest peak temperatures. In general, it was found that penetration for the 160-mm lens had the least sensitivity to process parameter variations. For example, it was found that for a 5% variation in peak power the 160-mm lens will yield a 0.3% variation in weld penetration, while the 120-mm lens and the 200-mm lens result in variations of 1.5% and 5.8%, respectively. In this manner, response surface equations can be utilized as an important indicator of process robustness.

Melting Efficiency and Travel Speed

The reason that the high peak power and low pulse energies were found to be effective in reducing battery temperatures can be explained by consideration of the melting efficiency. It is known (Ref. 14) that the two primary welding process variables that can increase the melting efficiency are the travel speed and the power.

Since average power was held constant in this experiment, an increase in the travel speed can be expected to reduce the heat input per length of weld. Certainly this will lower the peak temperatures in the battery. However, simply reducing the heat input per unit length of weld does not in itself increase the melting efficiency. Melting efficiency is only increased when less heat input is required for the same melt volume. One can observe increasing melting efficiency in this experiment by noting the decrease in battery temperatures along the constant penetration contours in Fig. 6. One can see that for the three lenses examined, welds of 0.2-mm penetration had peak temperatures that ranged from 113° to 70°C (235° to 158°F). This distinct example especially demonstrates the impact of melting efficiency.

Increasing pulse energy does not increase the melting efficiency because it

requires slower travel speeds. However, increasing peak power does lower battery temperatures and increase melting efficiency, because power is a primary melting efficiency variable. Higher power compresses the isotherms (Ref. 15) in the regions surrounding the weld and minimizes the heat conducted into the base metal.

Close examination of Table 1 reveals that the low-temperature welds, that is, those that were made at low pulse energies and high peak powers, required high travel speeds to maintain a consistent pulse overlap. Figure 8 illustrates the dramatic effect of weld travel speed on the average peak temperatures for all of the welds made in the experiment. One can clearly see that the primary process variable that affects the overall heat input to the part is the weld travel speed. Despite the substantial changes in the other process variables as shown in Table 1, only minor fluctuations about the fitted curve are apparent. Parameters such as pulse energy, pulse duration, pulse repetition rate, and the focused spot size, while they are arguably important, are not the process parameters that control the thermal gradients and therefore affect the melting efficiency. These results support the contention of Gornyi, *et al.* (Ref. 16), that pulsed LBW does not provide any theoretical advantage with respect to heat input.

The obvious conclusion one can draw from Fig. 8 is that high travel speeds are required in pulsed Nd:YAG LBW if the highest melting efficiencies are to be obtained. The dramatic effect of travel speed on melting efficiency has been demonstrated previously for many welding processes, including continuous power CO₂ LBW (Refs. 9, 17). It is not coincidental that many applications of CO₂ LBW that require low heat input are made at a high travel speed. Fast travel speeds are often required in high-volume manufacturing and are readily embraced when these high speeds are also found to reduce temperatures. For the manufacturing of pacemaker batteries as well, the increased production rate that results from a faster travel speed is an important bonus to the reduced temperatures that are realized.

It should also be mentioned that no greater propensity for solidification cracking was observed as a result of the faster cooling rates that must accompany an increased melting efficiency. While a

systematic study of the effect of process parameters on weld solidification cracking was not a goal of this experiment, the metallographic cross sections were all carefully examined, and no hot cracks were found in any of the welds.

Conclusions

1) Cardiac pacemaker batteries of 304L stainless steel have been welded in designed response surface experiments that varied the pulse energy, peak power, and lens focal length while yielding a requisite penetration depth of 0.2 mm with battery temperatures ranging from 65°C to 140°C.

2) Including increased peak power and lowered pulse energy, an optimized weld schedule was determined that reduced heat input to the battery and improved hermeticity via a wider fusion zone.

3) The significant reduction in battery temperature obtained for a given weld penetration is consistent with a change in the melting efficiency. Enhanced melting efficiencies were obtained by process conditions that increased the travel speed and the peak power.

4) Increases in beam irradiance, either by higher peak powers or smaller spot sizes, resulted in deeper and larger welds. These increases were attributed to enhanced absorption of the incident laser beam.

5) Low pulse energies in this application have been found to reduce battery temperatures because, for a constant average power, the resulting higher pulse frequencies and travel speeds lead to lower heat input per unit length of weld.

6) Weld fusion zone widths were found to widen as laser spot size was increased without expanding the overall cross-sectional area of the fusion zone.

Acknowledgments

The authors would like to thank Wilson Greatbatch Ltd. for supporting the publication of this work. We would also like to express our sincere appreciation to Jackie Page for her timely and excellent metallography, to Tim Rodameyer and Dave McCallum for their knowledgeable and conscientious experimental support, and to Charlie Robino for his careful review of the manuscript.

Portions of this work were funded by

the National Machine Tool Partnership and performed at Sandia National Laboratories, which is supported by the U.S. Department of Energy under contract number DE-ACO4-94AL85000.

References

1. Janssen, G. W. G. 1984. Laser welding in the manufacture of heart pacemakers. *Laser Weld, Cutting and Surface Treat*, TWI, Cambridge, England, pp. 33-35.
2. Cieslak, M. J., and Fuerschbach, P. W. 1988. On the weldability, composition, and hardness of pulsed and continuous Nd:YAG laser welds in Aluminum Alloys 6061, 5456, and 5086. *Metallurgical Transactions* 19B(4): 319-329.
3. Lippold, J. C. 1994. Solidification behavior and cracking susceptibility of pulsed laser welds in austenitic stainless steels. *Welding Journal* 73(6): 129-s to 139-s.
4. Watson, M. N. 1982. *Micro-spot Welding with a Pulsed Nd:YAG Laser*, TWI, Cambridge, England.
5. Engel, S. L. 1977. *1610 Application Guidelines*, GTE Sylvania.
6. Marshall, H. L. 1976. High power, high pulse rate YAG laser seam welding. *High Power Laser Technology*. SPIE, pp. 60-67.
7. Laserdyne. 1984. *Introduction to Laser Welding*, Laserdyne, Eden Prairie, Minn.
8. Liu, J. T., Weckman, D. C., and Kerr, H. W. 1993. The effects of process variables on pulsed Nd:YAG laser spot welds. *Metallurgical Transactions* 24B (Dec.): 1065-1076.
9. Fuerschbach, P. W. 1996. Measurement and prediction of energy transfer efficiency in laser beam welding. *Welding Journal* 75(1): 24-s to 34-s.
10. Box, G. E. P., Hunter, W. G., Hunter, J. S. 1978. *Statistics for Experimenters*, John Wiley and Sons.
11. Fuerschbach, P. W. 1987. Process control improvements in pulsed Nd:YAG laser closure welding of electromechanical relays. *International Power Beam Conference*. ASM, San Diego, Calif., pp. 157-164.
12. Nonhof, C. J. 1988. *Material Processing with Nd Lasers*. Electrochemical Publications Limited, Ayr, Scotland.
13. Kim, T. H., Albright, C. E., Chiang, S. 1990. The energy transfer efficiency in laser welding process. *Journal of Laser Applications* (Jan/Feb): 23-28.
14. Fuerschbach, P. W. 1991. Melting efficiency in fusion welding. *The Metal Science of Joining*. TMS, Cincinnati, Ohio, pp. 21-29.
15. Rykalin, N. N. 1951. *Calculation of Heat Flow in Welding*. Translated by Zvi Paley and C. M. Adams Jr., Moscow, Russia.
16. Gornyi, S. G., Lopota, V. A., Matyushin, I. V., Rudoi, I. G., Soroka, A. M. 1988. Comparison of the efficiency of heat input in laser welding. *Svar. Proiz.* (8): 31-32.
17. Okada, A. 1977. Application of melting efficiency and its problems. *J. of the Japan Welding Society* 46(2): 53-61.